

RESEARCH

Open Access



A novel camptothecin derivative, ZBH-01, exhibits superior antitumor efficacy than irinotecan by regulating the cell cycle

Yongqi Li^{1,2}, Dawei Zhao³, Wenqiu Zhang¹, Miaomiao Yang², Zhihui Wu², Weiguo Shi⁴, Shijie Lan¹, Zhen Guo¹, Hong Yu^{5*} and Di Wu^{1*} 

Abstract

Background Irinotecan (CPT-11) is a classic chemotherapeutic agent that plays an important role in the clinical treatment of metastatic colon cancer and other malignant tumors. We previously designed a series of novel irinotecan derivatives. In this study, we select one representative, ZBH-01, to investigate its sophisticated antitumor mechanism in colon tumor cells.

Methods The cytotoxic activity of ZBH-01 on colon cancer cells was evaluated by MTT or Cell Counting Kit-8 (CCK8) assay, 3D and xenograft model. The inhibitory effect of ZBH-01 on TOP1 was detected by DNA relaxation assay and Immuno Complex of Enzyme (ICE) bioassay. The molecular mechanism of ZBH-01 was explored by Next-Generation Sequencing (NGS), bioinformatics analyses, flow cytometry, qRT-PCR, and western blot etc.

Results ZBH-01 can induce obvious DNA damage and has superior antitumor activity against colon cancer cells compared to CPT-11 and SN38 (7-Ethyl-10-hydroxy camptothecin, the in vivo active form of CPT-11) both in vivo and in vitro. Its inhibitory effect on topoisomerase I (TOP1) was also comparable with these two control drugs. There are a much larger number of 842 downregulated and 927 upregulated mRNAs in ZBH-01 treatment group than that in the controls. The most significantly enriched KEGG pathways for these dysregulated mRNAs were DNA replication, the p53 signaling pathway, and the cell cycle. After constructing a protein–protein interaction (PPI) network and screening out a prominent cluster, 14 involved in the cell cycle process was identified. Consistently, ZBH-01 induced G₀/G₁ phase arrest in colon cancer cells, while CPT-11/SN38 caused S phase arrest. The initiation of apoptosis by ZBH-01 was also superior to CPT-11/SN38, followed by the increased expression of Bax, active caspase 3, and cleaved-PARP, and decreased expression of Bcl-2. Additionally, CCNA2 (cyclin A2), CDK2 (cyclin-dependent kinase 2), and MYBL2 (MYB proto-oncogene like 2) might be involved in the G₀/G₁ cell cycle arrest induced by ZBH-01.

Conclusions ZBH-01 can be an antitumor candidate drug for preclinical study in the future.

Keywords Irinotecan derivative ZBH-01, Colorectal cancer, Next-generation sequencing, Differentially expressed genes, Cell cycle, Apoptosis

*Correspondence:

Hong Yu

yhzhy@126.com

Di Wu

wudi1971@jlu.edu.cn

Full list of author information is available at the end of the article



© The Author(s) 2023. **Open Access** This article is licensed under a Creative Commons Attribution 4.0 International License, which permits use, sharing, adaptation, distribution and reproduction in any medium or format, as long as you give appropriate credit to the original author(s) and the source, provide a link to the Creative Commons licence, and indicate if changes were made. The images or other third party material in this article are included in the article's Creative Commons licence, unless indicated otherwise in a credit line to the material. If material is not included in the article's Creative Commons licence and your intended use is not permitted by statutory regulation or exceeds the permitted use, you will need to obtain permission directly from the copyright holder. To view a copy of this licence, visit <http://creativecommons.org/licenses/by/4.0/>. The Creative Commons Public Domain Dedication waiver (<http://creativecommons.org/publicdomain/zero/1.0/>) applies to the data made available in this article, unless otherwise stated in a credit line to the data.

Background

Colorectal cancer (CRC) is one of the main five cancer types and the five most common causes of cancer-related deaths in China, with the incidence and mortality are continuously increasing [1, 2]. Despite significant progress in precision medicine, Irinotecan (CPT-11) remains the primary chemotherapeutic agent for the treatment of metastatic CRC [3, 4].

CPT-11 is a camptothecin (CPT) analog, which was discovered from plant extracts more than 60 years ago. It disturbs the catalytic cycle of DNA TOP1 by stabilizing the reversible covalent enzyme–DNA cleavable complex. Moreover, by forming a drug–enzyme–DNA ternary complex during DNA synthesis, CPT-11 triggers the formation of irreversible single-stranded DNA break when the cleavable complex collides with the DNA replication fork [5]. This specific cytotoxic effect characterizes CPT-11 as a potent antitumor agent. However, its poor water solubility and serious side effects hinder its clinical applications. Until now, only two CPT analogs (irinotecan and topotecan) have been approved for cancer treatment

worldwide [6–8]. A breakthrough in the development of novel CPT analogs is still an urgent problem to be solved.

In the last 10 years, our group designed, synthesized, and characterized a series of novel irinotecan derivatives with higher antitumor activity and lower toxicity compared to CPT-11 [9–12]. However, their molecular mechanisms need to be precisely elucidated. This study explored the mechanism of one representative, ZBH-01, which showed a higher inhibitory effect on the development of colon tumors than CPT-11 preliminarily.

Materials and methods

Agents

ZBH-01 (Fig. 1A) was synthesized by the Institute of Pharmacology and Toxicology Academy of Military Medical Sciences (China). CPT-11 and SN38 (the activated form of irinotecan in vivo) were provided by the same institution. All chemical agents were dissolved in dimethyl sulfoxide (DMSO; Sigma-Aldrich, St. Louis, MO, USA) and stored at –80 °C before use.

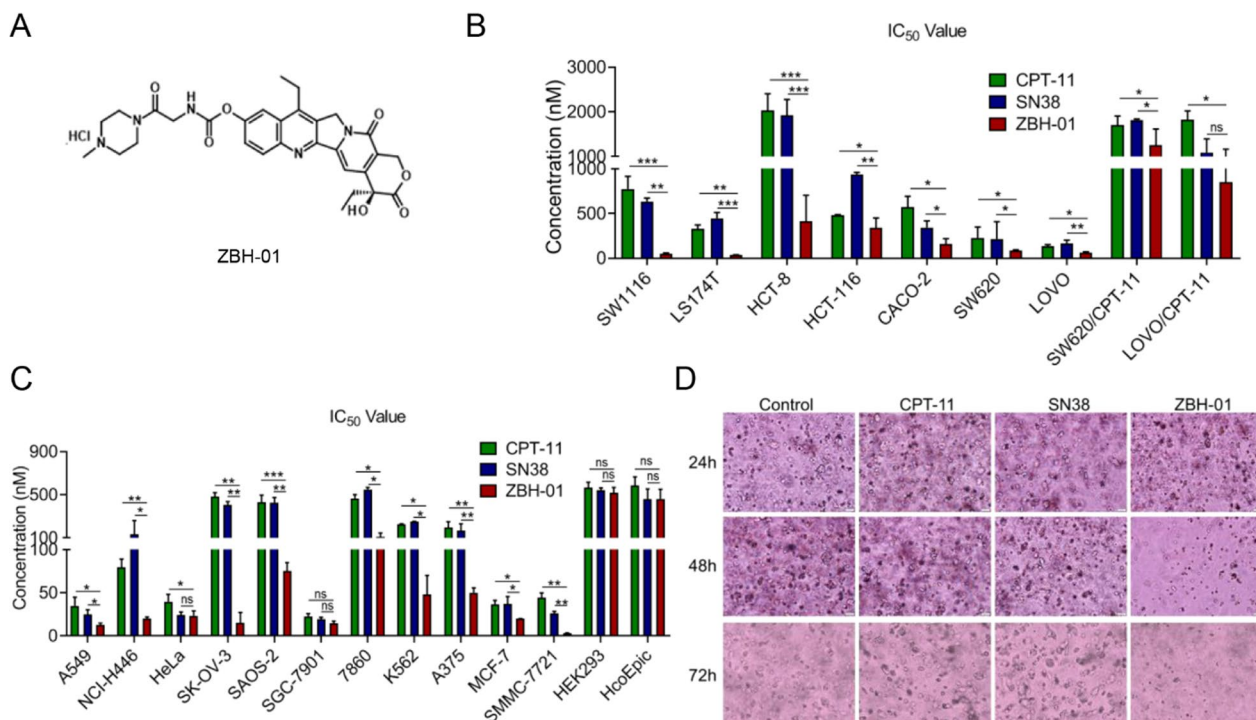


Fig. 1 Comparison of the anti-proliferation effects of ZBH-01, CPT-11, and SN38. **A** Chemical structural of ZBH-01. **B** The IC₅₀ values of ZBH-01, CPT-11, and SN38 in colorectal tumor cells and SW620/CPT-11 and LOVO/CPT-11 cells evaluated by MTT or CCK8 assay. **C** The IC₅₀ values of ZBH-01, CPT-11, and SN38 in non-colorectal tumor cells and HcoEpic and 293 cells evaluated by MTT or CCK8 assay. **D** The anti-tumorigenesis effects of ZBH-01, CPT-11, and SN38 in LS174T cells evaluated by 3D cell culture. The representative Images were captured by a fluorescence microscope (200×). ANOVA & two-tailed t-test, n = 3. *p < 0.05, **p < 0.01, ***p < 0.001. SW1116, LS174T, HCT-8, HCT-116, CACO-2, SW620 and LOVO, colon adenocarcinoma. A549 and NCI-H446, non-small cell lung cancer. HeLa, cervical carcinoma. SK-OV-3, ovarian cancer. SAOS-2, osteosarcoma. SGC-7901, gastric adenocarcinoma. 7860, renal carcinoma. K562, chronic myelogenous leukemia. A375, melanoma. MCF-7, breast cancer. SMMC-7721, hepatoma. HcoEpic, human colon mucosal epithelia. HEK293, human embryonic kidney cell

Cell lines

Eighteen human cancer cell lines including seven colon cancer cell lines and two CPT-11-resistant colorectal cancer cell lines SW620/CPT-11 and LOVO/CPT-11, a normal human colon mucosal epithelial cell lines (HcoEpic), and the human HEK293 cell lines were maintained in DDM or RPMI 1640 media (Life Technologies, Grand Island, NY, USA) supplemented with 10% fetal bovine serum (FBS, Gibco), 2 mmol/l glutamine, 100 U/ml penicillin, and 100 µg/ml streptomycin in a humidified incubator at 37 °C and 5% CO₂.

Cell viability assay in vitro

The cytotoxic activity of ZBH-01 was evaluated against the above cell lines using MTT or Cell Counting Kit-8 (CCK8) assay as previously described [9, 11]. HEK293 and HcoEpic cells were used as control cells. The different cell lines, including the colon cancer cell lines, were treated with different concentrations of ZBH-01, CPT-11, and SN38. After 72 h of incubation, the absorbance of cells in each group was measured at 450 nm using a spectrophotometer. The IC₅₀ values (50% inhibition of cell growth) were calculated by Statistical Product and Service Solutions (SPSS) 23.0.

3D culture

Hydrogel (The Well Bioscience, Shanghai, China) was mixed with cell culture medium to form a hydrogel matrix with the dilution ratio 1:2 v/v. Then the hydrogel matrix and LS174T cells were uniformly mixed and were seeded into a six-well plate at 1 × 10⁶ cells/ml. The medium was added to cover the hydrogel carefully. Afterwards, cells were treated with 50 nmol/L ZBH-01, CPT-11, and SN38 for 24–72 h, respectively. Images were captured using a fluorescence microscope (Olympus IX51, Tokyo, Japan).

DNA relaxation assay

The DNA relaxation assay was performed according to the manufacturer's instructions (TopoGEN, Inc., Port Orange, FL, USA) [11]. The reaction was conducted in a dosage-dependent manner. We also performed qRT-PCR and western blot to evaluate the inhibition of ZBH-01 on TOP1 in LS174T or SW1116 colon cancer cells. The primers of TOP1 (DHS626257) were provided by XYbiotech (Shanghai, China). The forward (5'-CTA CCTCATGAAGATCCTCACCGA-3') and reverse (5'-TTCTCCTTAATGTCACGCACGATT-3') primers of β-actin were provided by Shanghai Generay Biotech Co., Ltd. Total RNA isolation, first-strand cDNA

synthesis, and the qRT-PCR assay was performed as described below (see qRT-PCR assay section) [13].

Immuno complex of enzyme (ICE) bioassay

To detect the alteration of the covalent TOP1-DNA complex in colon cancer cells after ZBH-01 treatment, the TOP1-DNA adducts were isolated by the in vivo complex of enzyme (ICE) bioassay [14]. Briefly, 1 × 10⁶ treated or untreated LS174T cells were lysed with 1 ml of 1% sarkosyl. After homogenization by a Dounce homogenizer, cell lysates were gently layered on four step gradients CsCl solutions with densities of 1.82, 1.72, 1.50, and 1.45 (2 ml of each). Then the tubes were centrifuged at 165,000 g for 24 h at 20 °C. Next, half-milliliter fractions were collected from the bottom of the tubes. Aliquots of each fraction (100 µl) were diluted with an equal volume of 25 mM sodium phosphate buffer (pH 6.5) and applied to Immobilon-P membranes (Millipore) by a slot-blot vacuum manifold. The topoisomerase-DNA adducts were detected by western blot with a anti-TOP1 mAb.

next-generation sequencing (NGS)

First, LS174T cells were subjected to 50 nmol/L ZBH-01, CPT-11, and SN38 for 24 h. Total RNA was extracted using TRIzol reagent (Invitrogen, CA, USA) following the manufacturer's instructions. Total RNA quantity and purity were analyzed by Bioanalyzer 2100 and RNA 6000 Nano Lab Chip Kit (Agilent, CA, USA) with RIN number > 7.0. Then, 3 µg RNA per sample was used to prepare RNA-Seq libraries. Sequencing libraries were generated using NEBNext Ultra II RNA Library Prep Kit for Illumina (NEB, E7760) following the manufacturer's recommendations. The PCR was performed with Phusion High-Fidelity DNA polymerase, universal PCR primers, and index (X) Primer. Finally, PCR products were purified (AMPure XP system) and library quality was assessed on the Agilent Bioanalyzer 2100 system. Paired-end sequencing was performed using Illumina HiSeq X Ten (Illumina, San Diego, CA). Raw data (raw reads) in the fastq format were processed by the Fastp software. All downstream analyses were based on clean high-quality data. Paired-end clean reads were aligned to the reference genome using STAR V20201. Cufflinks v2.2.1 was used to count the number of reads mapped to each gene. The FPKM of each gene was calculated based on the length of the gene and the count of reads mapped to this gene. The resulting *p*-values were adjusted using Benjamini and Hochberg's approach for controlling the false discovery rate (FDR).

Differential expression analysis of mRNAs

To compare mRNA expression differences among ZBH-01, CPT-11, and SN38 groups, a *p*-value < 0.05 and |log₂

fold change > 1 were set as the threshold for significantly differential expressions. First, the gene expression profiles of the three groups were compared to the control group. Then the three datasets obtained were analyzed together to obtain commonly expressed genes and a ZBH-01 group-specific differentially expressed gene list.

Bioinformatics analyses

Gene Ontology (GO) classifications (biological process, cellular component, and molecular function) and the Kyoto Encyclopedia of Genes and Genomes (KEGG) pathway enrichment analyses were hierarchically investigated using 'clusterProfiler' in R 3.4.0 (R Foundation, Vienna, Austria) [15] and KEGG Pathway Database (<http://www.genome.jp/kegg/pathway.html>). The proteins encoded by upregulated and downregulated differentially expressed mRNAs (DEmRNAs) in the ZBH-01 group were used to construct a PPI network using STRING (<https://string-db.org/>) and Cytoscape 3.5.1 (<http://www.cytoscape.org/>, The Cytoscape Consortium, San Diego, CA, USA) [16, 17]. We used Cytotype MCODE to identify key network modules and select hub genes.

qRT-PCR assay

The PCR primers of some genes are shown in Table 1. Besides, the primers of other genes were provided by XYbiotech (Shanghai, China) including BUB1 (catalog number. DHS322648), BUB1B (DHS646748), CCNA2 (DHS819739), CDC20 (DHS889533), CDC25C (DHS740393), CDC45 (DHS793726), CDC7 (DHS095090), CDK2 (DHS278875), CHEK1 (DHS670983), E2F8 (DHS048256), EZF2 (DHS068552), FOXM1 (DHS718140), MCM3 (DHS061267), MCM7 (DHS794915), MYBL2 (DHS516386), ORC1 (DHS500377), PKMYT1 (DHS687810), RAD54L (DHS609809), TOP2A (DHS036498), and TTK (DHS713780). Total RNA isolation was performed with the EasyPure RNA kit (Transgen) according to the manufacturer's guidelines. RNA concentrations were measured by a microplate reader (BioTek Synergy H1). The TransScript All-in-One First-Strand cDNA Synthesis SuperMix for qPCR kit was used for reverse transcription according to the manufacturer's instructions. The 20 μ L reaction volumes contained 1 μ g RNA prepared by combining 4 μ L transcript all-in-one supermix for qPCR, 1 μ L gDNA remover, and variable RNase-free water. The reverse transcription reactions were performed for 15 min

Table 1 Primers for qRT-PCR

Genes	Forward primer (5'-3')	Reverse primer (5'-3')
MCL1	TCTCATTCTTTTGGTGCCCTTG	TAAC TAGCCAGTC(TGTTTTGTC
XIAP	GTGAATGCTCAGAAAGACAGTATGC	TGTCCACAAGGAACAAAACGATAG
BIRC3	GATGCTGGATAACTGGAAAAGAG	TGAAGAAGGAAAAGTAGGCTGAG
MDMX	ATTTTCCTTTTCAGGTATGGC	AGGTA CTGTTTTCGTTGTTGG
MDM2	AAGGGAAGAAACCCAAGACAAAGA	GCACATGTAAAGCAGGCCATAAGA
CYC	TGATGCCTTTGTCTTATTGG	TTTATTATGAAGTGTCCAGTG
APAF-1	ATCTGGGCTTCTGATGAACTGC	CAACACCCAAGAGTCCCAAACAT
CASP9	AGCCAACCTAGAAAACCTTACC	TCACCAATCTCCAGAACCAAT
cBid	GTCACACGCCGCTCTTGCT	CTGTCCGTTCCAGTCCATCCATT
BAX	AGGATGCGTCCACCAAGAAGC	GGCAAAGTAGAAAAGGGCGACA
BCL-XL	GAGAATCACTAACCAGAGACGAGA	GGAGAGAAAGTCAACCACCAGC
PTEN	TAAGGACCAGAGACAAAAGGGA	GGCAGACCACAACTGAGGATT
CDK6	TGATCAACTAGGAAAAATCTTGAC	GGCAACTCTCTAGGCCAGT
NEK2	TGTCTCTGGCAAGTAATCCAG	CAGGTCCTTGCACTTGGACT
CCND1	AGCTGTGCATCTACACCGAC	TGTGAGGCGGTAGTAGGACA
CCNE2	ACCTCATTATTCATTGCTTCCAA	TCTTCACTGCAAGCACCATC
BIRC5	TTCTCAGTGGGGCAGTGGATG	TTTCTCAAGGACCACCGCATCT
CDK4	CTTCTGCAGTCCACATATGCAACA	CAACTGGTCGGCTTCAGAGTTTC
P53	AGCTTTGAGGTGCGTGTTTGTG	TCTCCATCCAGTGGTTTCTTCTTTG
RB1	CACAACCCAGCAGTTCAATATC	TGAGATCACCAGATCATCTTCC
ATM	TGTGACTTTTTCAGGGGATTTG	ATAGGAATCAGGGCTTTTGGGA
ATR	GGGAATCACGACTCGCTGAA	CTAGTAGCATAGCTGCACCATGGA
XAF1	GCCTACTTGCTGTGGTGGTCTTGT	ACGCCTGGTTTGTGAGGGTTTT
P21	TAAACAAAAACTAGCGGTTGA	AGGAGAACACGGGATGAGGA
CASP3	TGGCATTGAGACAGACA	GGCACAAGCGACTG

at 42 °C and 5 s at 85 °C. Each reverse transcription product was diluted 10 times by adding 180 μL H₂O to 20 μL cDNA. The qPCR with TransStart Tip Green qPCR Super-Mix kit (Transgen) was also performed according to the manufacturer's protocol. Briefly, 20 μL reaction volume were prepared by combining 10 μL transstart tip green qPCR supermix, 0.4 μL passive reference dye, 0.5 μL forward primer and 0.5 μL reverse primer, 3 μL cDNA and 5.6 μL ddH₂O. The cycling conditions were: 94 °C for 30 s, 40 cycles at 94 °C for 5 s, and 60 °C for 30 s. The relative gene expression data were analyzed by the $2^{-\Delta\Delta CT}$ method.

Flow cytometry

To analyze the changes in the cell cycle, cell apoptosis, and mitochondrial membrane potential (MMP), SW1116 and LS174T colon cancer cells were harvested after exposure to 50 nmol/L ZBH-01, CPT-11, and SN38 for 12–72 h. Then, cells were stained by FxCycle™ PI/RNase Staining Solution (Invitrogen), FITC Annexin V Apoptosis Detection kit I (BD Biosciences, San Diego, CA, USA), and Mitochondrial Membrane Potential Detection Kit (BD Biosciences, San Diego, CA, USA) according to the manufacturer's protocol. Flow cytometry was performed using a FACS Calibur system (BD Dickinson). A minimum of 10,000 events was recorded for each sample. Data were acquired and analyzed by CellQuest (BD Biosciences), ModFit 4.0 (BD Biosciences), and FlowJo (TreeStar, Inc., Ashland, OR) software [11].

Western blot

First, SW1116 and LS174T cells were seeded in 6-well plates with a complete medium as previously described [9]. After cultivation for 24 h, cells were treated with 50 nmol/L ZBH-01, CPT-11, and SN38 for 48 h and harvested. Next, cell pellets were lysed and the protein concentrations of each sample were measured. Then, samples were separated by 10% SDS-PAGE and transferred to a polyvinylidene difluoride membrane (GE Healthcare, Piscataway, NJ). Samples were incubated with corresponding primary antibodies (1:500–1000 dilution) in 5% BSA at 4 °C overnight. Then, the membrane was washed and incubated with appropriate secondary antibodies at room temperature for 1 h. The antibodies included TOP1, caspase 3, PARP, P53, Bax, Bcl-xL (54H6), p-BRCA1, p-H2AX, p-CHK1, p-CHK2, p-P53 (Cell Signaling Technology, Shanghai, China). β-actin was used as the internal reference (1:5000 dilution). Protein bands were visualized with ECLplus Western Blotting Detection Reagents (GE Healthcare) on the ECL System (Millipore, Billerica, MA) [11].

Antitumor activity of ZBH-01 in vivo

The antitumor activity in vivo was evaluated using 6–8 week-old female nude mice as previously described [10] in accordance with the Aimal Experimental Guidelines of Jilin University. The xenografts model was established by subcutaneous injection of 1×10^6 LS174T cells in the left flank. Tumor growths were measured with vernier calipers twice a week. When masses reached 100–150 mm³, mice were randomly assigned to the treatment (n=6) or control (n=6, treated with saline) groups. Mice in the treatment group intravenously (i.v.) received ZBH-01 (40 mg/kg) or CPT-11 (40 mg/kg) using the q4dx3w schedule [18, 19]. Animals were treated for 21 d, monitored twice a week for signs of toxicity, and weighed every 3 d. At the end of the experiment, all mice were euthanized. Their main organs such as the heart, liver, spleen, lung, kidney and tumor tissues were stripped. Tissue sections were prepared and stained with hematoxylin and eosin (H&E) according to standard protocol. Tumor volume and growth inhibition were calculated [20]. Tumor volume (TV) = length × width² / 2; Relative tumor volume (RTV) = TV_t / TV₀ (TV_t: tumor volume at day t, TV₀: tumor volume at the initiation of treatment); Relative tumor proliferation (T/C) = RTV_t / RTV_C × 100% (RTV_t: the treatment group RTV, RTV_C: the control group RTV). To detect tumor cell apoptosis induced by ZBH-01 in vivo, fresh tumor tissues were dissected into small pieces and crushed by the flat end of the plunger of sterile syringe. Cell suspensions were then filtered and centrifuged for 10 min 1200 g, 4 °C. Afterwards, each sample was stained by FITC-Annexin V/PI as described in the previous Sect. “Flow cytometry”.

Statistical analyses

Data are expressed as means ± standard deviations (SDs). One-way analysis of variance (ANOVA), χ^2 test, the two-tailed Student's *t*-test, or Mann–Whitney *U* test was performed using SPSS 23.0 software (SPSS, Inc., Chicago, IL, USA) and GraphPad Prism version 8.01 (GraphPad Software, San Diego, CA, USA). A *p* < 0.05 was considered statistically significant.

Results

ZBH-01 showed superior antitumor effects than CPT-11 and SN38

CPT-11 is a prodrug and SN38 represents its metabolically-activated form in vivo. Therefore, we used CPT-11 or SN38 as positive controls in our study. We evaluate the anti-proliferation effect of ZBH-01 on multiple tumor cell lines derived from different origins. The results showed that the IC₅₀ values of ZBH-01 are significantly lower than that of CPT-11 and SN38 in most tumor cell

lines, even in the two CPT-11 resistant colorectal cancer cell lines SW620/CPT-11 and LOVO/CPT-11 (Fig. 1B, C). More prominently, the IC₅₀ value of ZBH-01 is comparable with that of CPT-11 and SN38 in normal epithelial HcoEpic cells and 293 cells. In addition, the result of 3D cell culture further verified the superior anti-tumorigenesis effect of ZBH-01 (Fig. 1D). Altogether, ZBH-01 showed higher anti-proliferative effect as compare to CPT-11 and SN38. We selected LS174T and SW1116 cells for subsequent experiments. The IC₅₀ value of ZBH-01 on the two cell lines is about 50 nmol/L.

The reduction of TOP1 activity by ZBH-01 is weaker compared to CPT-11 and SN38

By forming a drug–enzyme–DNA complex, the drug prevents the relegation step normally catalyzed by topoisomerase, finally inhibiting the relaxation activity. Hence, to explore the interaction of ZBH-01 and TOP1, we performed a DNA relaxation assay. The inhibitory effect of ZBH-01 on TOP1 was weaker than CPT-11 and SN38 (Fig. 2A). This result was contradictory to our previous reports [9, 11], which might indicate the heterogeneity and complexity of ZBH-01 mechanisms. Nevertheless, after treatment with 50 nmol/L ZBH-01 for 24 h, LS174T cells presented decreased protein levels of TOP1 (Fig. 9), while its mRNA levels were not suppressed (Fig. 5). This result was consistent with previous studies, indicating a significant downregulation of TOP1 in tumor cells treated with topoisomerase inhibitors [19, 20]. The reasons for our conflicting results remain to be further elucidated.

ZBH-01 mediated TOP1 trapping in LS174T cells was measured by the ICE bioassay, which can detect the covalently link of TOP1 to genomic DNA after drug treatment. As expected, the result of immunoblot showed that the signals of TOP1 band in the DNA-containing fractions in ZBH-01-treated cells were more enhanced than that in CPT-11- and SN38-treated cells (Fig. 2B). This result further verify the inhibitory ability of ZBH-01 to TOP1 through chromatin-associated TOP cleavage complexes.

ZBH-01 treatment leads to the highest number of DEmRNAs in LS174T cells compared to CPT-11 and SN38

Previous studies have identified hundreds of abnormally expressed protein-coding genes in tumor cells after treatment with various drugs [21, 22]. Additionally, the gene expression profile of colon cancer cells can be used to predict and distinguish the response to multiple chemotherapeutic agents [23]. Hence, we used NGS to analyze expression changes in LS174T cells in response to ZBH-01 treatment. After performing the t-test, we used $p < 0.05$ and $|\text{Log}_2 \text{ fold change}| > 1$ as criteria to screen out 2072 DEmRNAs (1026 downregulated and 1046 upregulated) between ZBH-01 and controls; 380 DEmRNAs (251 downregulated and 129 upregulated) between CPT-11 and the control group; and 377 DEmRNAs (215 downregulated and 162 upregulated) between SN38 and controls. The Venn diagrams were used to classify the DEmRNAs among ZBH-01, CPT-11, and SN38 groups (Fig. 3A, B). The three groups shared 100 DEmRNAs (62 downregulated and 38 upregulated mRNAs). Compared

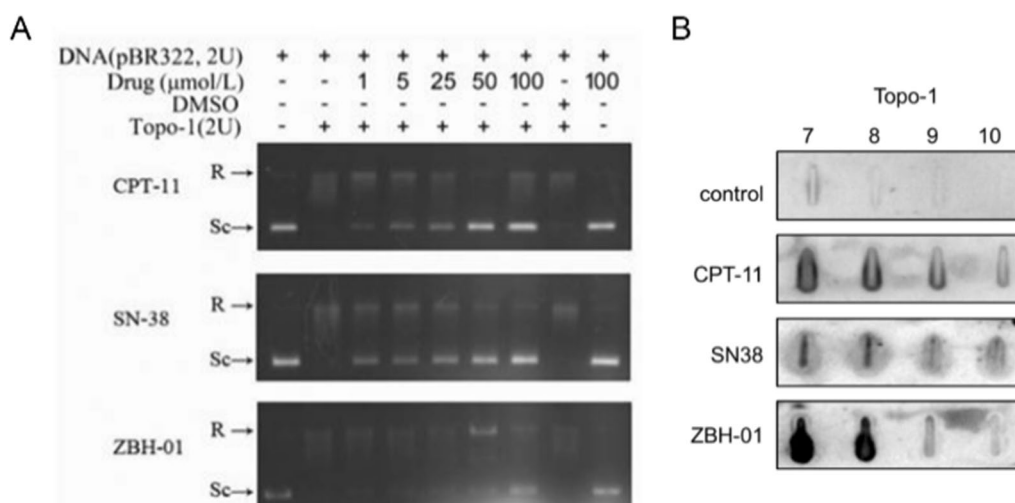


Fig. 2 Inhibitory effect of ZBH-01 on TOP1. **A** TOP1-catalyzed DNA relaxation was inhibited by CPT-11, SN-38, and ZBH-01. The DNA strand breakage induced by TOP1 was evaluated by the conversion of the double-stranded supercoiled DNA to a relaxed form. The position of supercoiled DNA (Sc) and relaxed DNA (R) are indicated. **B** The image of immunoblot showed the signals of TOP1 band in the DNA-containing fractions in LS174T cells after treatment with ZBH-01, CPT-11, and SN38. The fractions are indicated by numbers

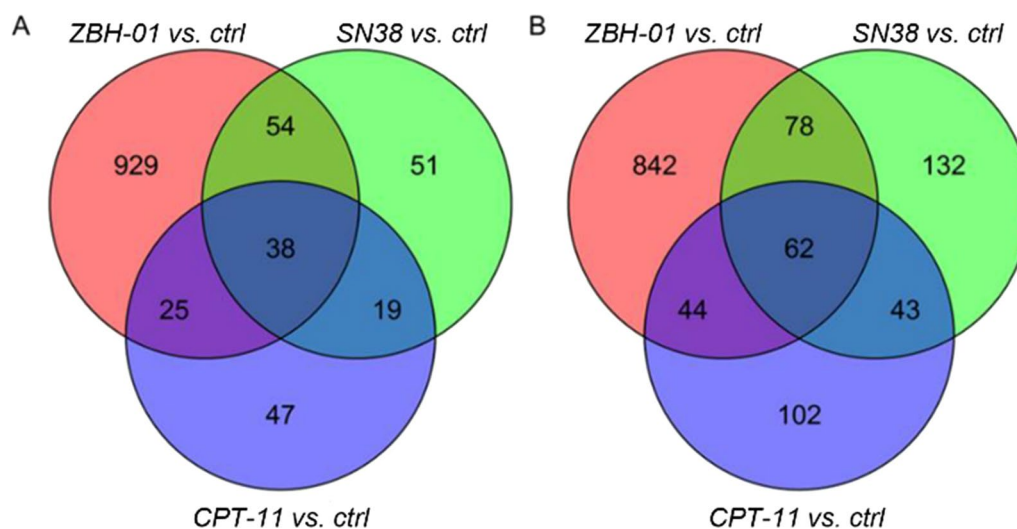


Fig. 3 Venn diagrams for differentially expressed genes among ZBH-01, CPT-11, and SN38 groups. **A** Upregulated genes; **B** Downregulated genes

to CPT-11 and SN38, the ZBH-01-treated group presented 1769 DEmRNAs (842 downregulated and 927 upregulated mRNAs). These results suggested that ZBH-01 might have a unique anti-tumor mechanism.

Clustering of specific GO items and KEGG pathways in the ZBH-01-treated group

Next, we performed GO enrichment analysis using 1769 DEmRNAs specific to the ZBH-01 group. The DEmRNAs were classified regarding their molecular functions (MF), biological processes (BP), and cellular components (CC). For BP (Fig. 4A), the DEmRNAs were mainly enriched in sister chromatid segregation, DNA-dependent DNA replication, and chromosome segregation. For CC (Fig. 4B), the DEmRNAs were mainly enriched in the chromosomal region, condensed chromosome, and spindle. Regarding MF (Fig. 4C), the DEmRNAs were mainly enriched in catalytic activity, acting on DNA, DNA-dependent ATPase activity, and DNA-secondary structure binding. The KEGG pathway results revealed that most ZBH-01 group-specific DEmRNAs were clustered in DNA replication, p53 signaling pathway, and cell cycle (Fig. 4D).

The proteins encoded by DEmRNAs specific to the ZBH-01 group were prominently involved in cell cycle regulation

We constructed a PPI network (Fig. 5A) based on the proteins encoded by ZBH-01 group-specific DEmRNAs using the STRING database (<http://string-db.org>) [24]. Then one prominent module (score=61.833) were filtered out from the PPI network using Cytotype MCODE (Fig. 5B) [25]. This module consists of 73 downregulated genes. We conducted enrichment analysis again with these 73 genes demonstrating that they were principally

associated with cell cycle, progesterone-mediated oocyte maturation, and oocyte meiosis. Fourteen genes (CDC45, CDC20, BUB1, CCNA2, BUB1B, TTK, CHEK1, CDC25C, MCM3, MCM7, ORC1, CDK2, CDC7, and PKMYT1) were involved in the most enriched cell cycle pathway (Fig. 5C). Their expression was further verified by qRT-PCR (Fig. 5D). It is noteworthy that among these 14 cell cycle-related genes, the interaction between transcription factor MYB proto-oncogene like 2 (MYBL2) and cyclin A2 (CCNA2)/cyclin dependent kinase 2 (CDK2) plays a decisive role in the cell cycle transition from the G₁ to the S phase [26–32]. So we detected their expression by western blot. The result demonstrated that MYBL2, CCNA2, and CDK2 level were repressed in ZBH-01 group compared to CPT-11 and SN38 group (Fig. 5E). Whether these genes are the potential target of ZBH-01 and the more precise interaction between them during ZBH-01 treatment needs to be further studied.

Interestingly, we found that TOP2A is in the center of the module. In the relaxation assay results, we observed that the inhibition of ZBH-01 on TOP1 was weaker than CPT-11 and SN38. Thus, we need to further explore whether TOP2A is also a target of ZBH-01. Other key genes were also included in the module, such as FOXM1, RAD54L, UHRF1, MYBL2, EZH2, and E2F8, and play important roles in regulating the cell cycle.

Relative expression of some ZBH-01 group-specific DEmRNAs by qRT-PCR

Next, we selected some genes in Fig. 5B to perform qRT-PCR. These genes included not only the aforementioned DEmRNAs, but also classical genes involved in the cell cycle, DNA replication, and apoptosis regulation because

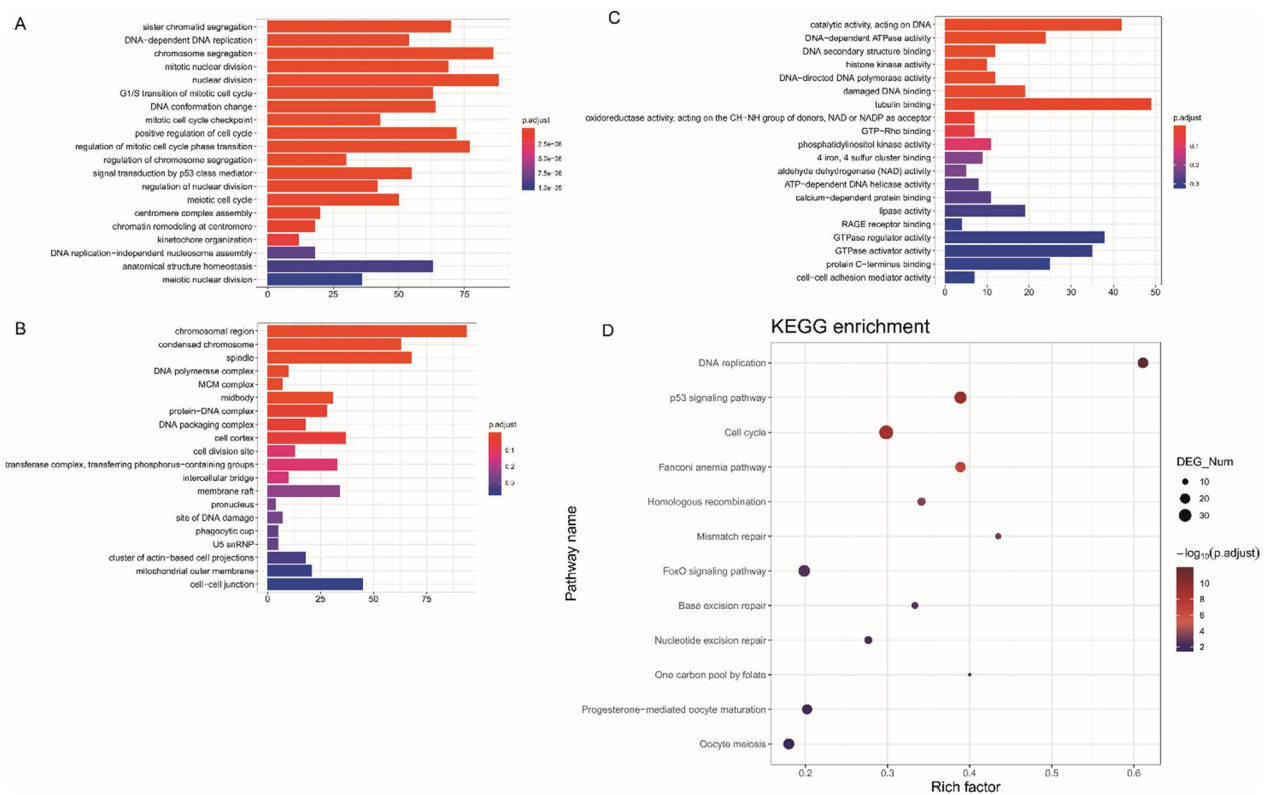


Fig. 4 Significantly enriched GO terms and KEGG pathways for the DEmRNAs in the ZBH-01-treated group. **A** Biological processes (BP). **B** Cellular components (CC). **C** Molecular functions (MF). **D** KEGG pathways

they play important roles in CPT-11 anti-tumor process as reported by our group and others [3, 6, 9, 11, 22]. The results demonstrated that the expression trend of most genes was consistent with the bioinformatics data and our previous report (Figs. 5D, 8).

ZBH-01 induces G₀/G₁-phase arrest and increased apoptosis in colon cancer cells

The above results showed that the gene expression features of LS174T cells treated with ZBH-01 were significantly altered compared to CPT-11 and SN38 groups. Most DEmRNAs were mainly involved in DNA replication, cell cycle, and P53 signal pathway. Thus, we evaluated the effects of ZBH-01 on the cell cycle and apoptosis by two colon cancer cell lines (LS174T and SW1116). The results showed that ZBH-01 preferably arrested tumor cells in the G₀/G₁ phase, while CPT-11 and SN38 arrested cells in the S phase (Fig. 6). Regarding apoptosis, ZBH-01 induced more apoptosis and necrosis than CPT-11 and SN38 (Fig. 7). These results are in accord with Fig. 5E. The more exact molecular mechanism is worthy of elucidation in the future.

The cells' ability to undergo apoptosis can be a major determinant of drug sensitivity [22]. Thus, to

further analyze the effects of ZBH-01 on cell apoptosis, we detected the changes in mitochondrial membrane potential (MMP) in LS174T cells after drug treatment. The results showed that the MMP of the ZBH-01 group was significantly higher than CPT-11 and SN38 groups. We further verified the expression of some genes related to apoptosis using qRT-PCR, although they were not in the selected module of the PPI network. Some genes, including APAF1, ATR, BAX, BIRC3, CCND1, CCNE2, CDK4, CDK6, CDKN1A, MCL1, MDM2, and NEK2 showed consistent expression trends with the NGS result; while other genes, including ATM, BCL2L1, BID, BIRC5, CASP3, CASP9, CYCS, MDM4, RB1, TP53, TEP1, XAF1, and XIAP, displayed inconsistent expression trends (Fig. 8).

ZBH-01 alters the expression of some key proteins related to cell apoptosis and DNA damage in colon cancer cells

The aforementioned Fig 5E showed that ZBH-01 induced abnormal expression of several cell cycle-related genes. Here the expression changes of some key proteins related to apoptosis and DNA damage induced by ZBH-01 were similarly analyzed by western blot assay. The results showed that after treatment with 50 nmol/L ZBH-01, the

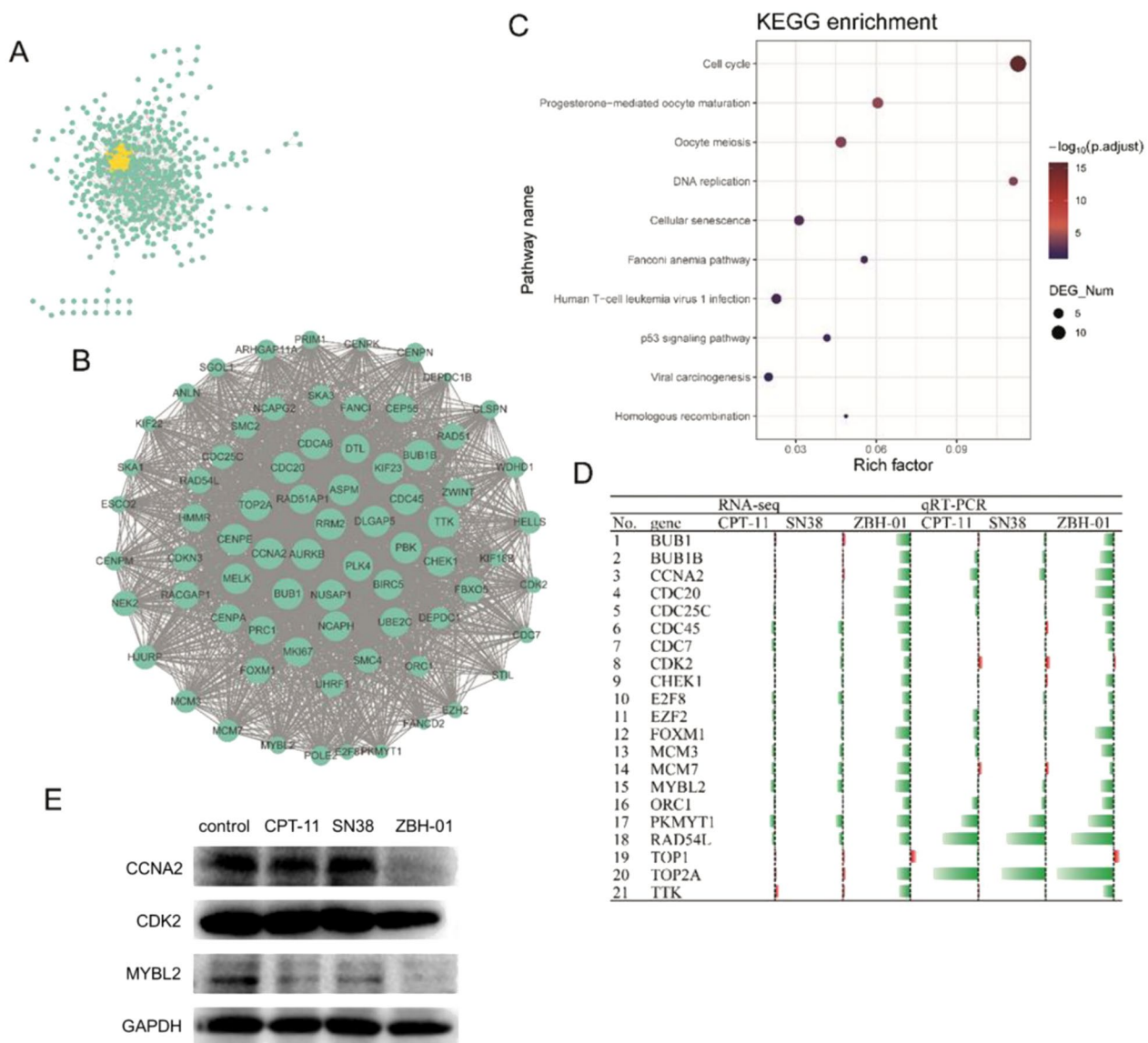


Fig. 5 The proteins encoded by ZBH-01 group-specific DE mRNAs were prominently involved in cell cycle regulation **A**. The PPI network. The yellow part highlights the most prominent module. **B** Enlargement of the yellow module in **(A)**, containing 73 genes. **C** Most significantly enriched KEGG pathway of these 73 genes. **D** qRT-PCR result showed the relative expression of some DE mRNAs in **(B)** in LS174T cells after treatment with 50 nmol/l ZBH-01, CPT-11, and SN38 24 h (logarithmic transformation). Green: downregulated; Red: upregulated. **E**, The result of western blot showed that ZBH-01 is more efficient than CPT-11 and SN38 in regulating the expression of three representative cell cycle related genes, MYBL2, CCNA2, and CDK2

level of cleaved-Cas3 and cleaved-PARP is both higher than that in CPT-11 and SN38 group (Fig 9A). CPT-11 and SN38 treatment exhibits comparable activity at the same condition. The Bax gene encodes a protein that promotes cell apoptosis, while another protein Bcl-xL can form heterodimer with other pro-apoptotic proteins to inhibit cell apoptosis. ZBH-01 presented higher effects on upregulation of Bax expression and downregulation of Bcl-xL level than CPT-11 and SN38 (Fig 9B). In addition,

the level of activated caspase 3 in ZBH-01 group were significantly higher compare to CPT-11 and SN38 group (Fig 9C, D).

To characterize the DNA damage response during ZBH-01 treatment, the activation status and expression levels of proteins involved in DNA damage checkpoint pathways were measured in LS174T cells (Fig 9B). Among them, γ -H2AX and BRCA1 is the mediator of DNA damage, CHK1 and CHK2 is the transducer of DNA damage,

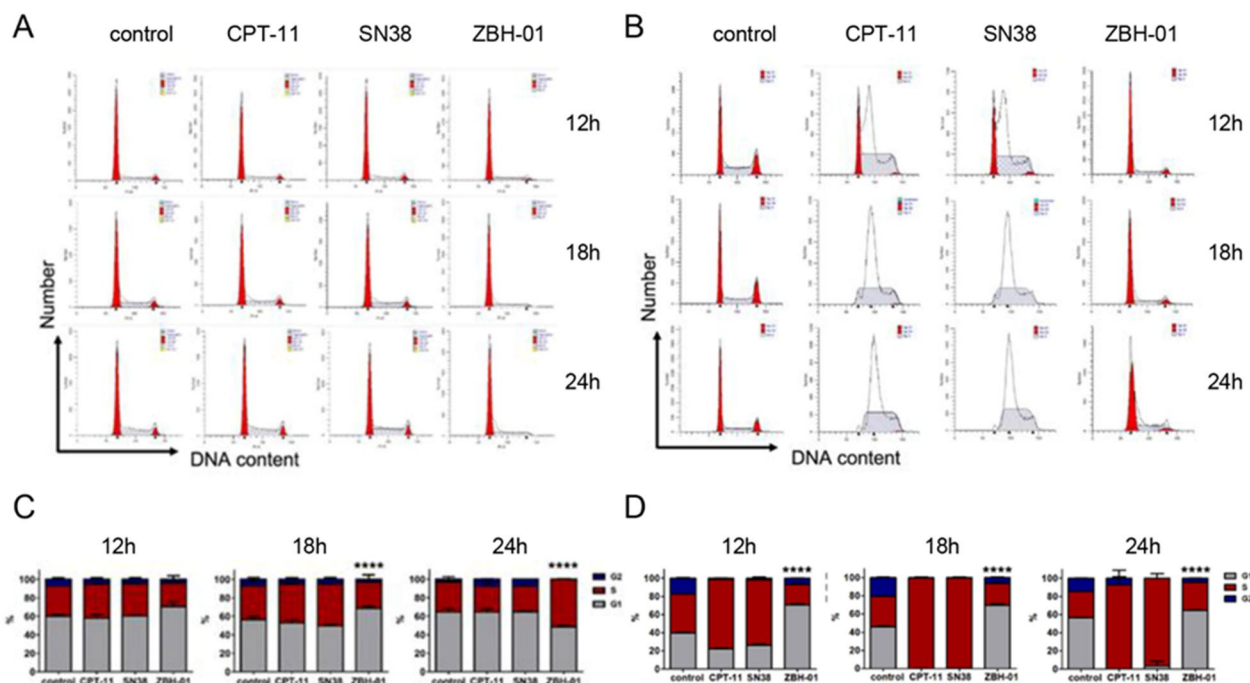


Fig. 6 Cell cycle alteration in response to drug treatments. LS174T and SW1116 cells were treated with 50 nmol/l ZBH-01, CPT-11, and SN38 for 12, 18, and 24 h. The percentage of cells in G₀/G₁, S, and G₂/M phases were analyzed by flow cytometry. **A** Histograms of cell cycle distribution of LS174T cells at different time points. **B** Statistical analysis of A. 12 h: $\chi^2=7.5391$, $p=0.2738$; 18 h: $\chi^2=40.6417$, **** $p<0.0001$; 24 h: $\chi^2=60.8731$, **** $p<0.0001$. **C** Histograms of cell cycle distribution of SW1116 cells at different times. **D** Statistical analysis of C. 12 h: $\chi^2=96.9852$, **** $p<0.0001$; 18 h: $\chi^2=242.4146$, **** $p<0.0001$; 24 h: $\chi^2=197.4546$, **** $p<0.0001$. ANOVA & two-tailed t-test, $n=3$

and P53 is the effector of DNA damage [20]. The results showed that ZBH-01 treatment increased the expression of p-BRCA1, p-H2AX, p-CHK1, p-CHK2, and p-P53 as compare with CPT-11 and SN38, which indicates that ZBH-01 promises more efficient activity in DNA damage. Altogether, these results suggested that ZBH-01 induced cell cycle arrest and apoptosis probably through generating more extent of DNA damage.

ZBH-01 represses tumor growth of colon cancer in vivo.

Xenografts models derived from LS174T cells were used to evaluate the antitumor effects of ZBH-01 and CPT-11 in vivo. Compared to controls, tumor growth was significantly suppressed in CPT-11- and ZBH-01-treated groups (Fig. 10A, C). The dosage of ZBH-01 seemed to cause a lighter loss of body weight than CPT-11, but was still significantly lower than the average weight of the control group (Fig. 10B). There was no significant difference in the rate of relative tumor proliferation between ZBH-01 and CPT-11 group (Fig. 10D). Nevertheless, the relative tumor volume was significantly lower in ZBH-01 group than in the control group, but not in the CPT-11 group. ZBH-01 induced a higher percentage of tumor cell apoptosis than CPT-11 (Fig. 10E, F). The results of H&E staining showed that ZBH-01 has good tolerable

toxicities in vivo (Fig. 10G). The morphology and structures of the main organs, such as the heart, liver, spleen, lung, and kidney in ZBH-01-treated mice are all exhibited no apparent pathological abnormalities.

Discussion

DNA topoisomerases, which can be divided into TOP1 and TOP2, are a class of enzymes that control the topological state of DNA through catalyzing the break and combination of DNA strands. Topoisomerase inhibitors are an important class of anti-tumor drugs since tumor cells have abnormally high expression of TOP1 and TOP2 [33]. Irinotecan (CPT-11) is a TOP1 inhibitor [34], which plays an important role in clinical treatment of metastatic colorectal cancer [35].

In the last three decades, many groups synthesized CPT-11 derivatives to enhance their cytotoxicity or minimize adverse events [18, 36, 37], but no new analogs have been approved so far. We synthesized a novel CPT-11 derivative ZBH-01 using a natural amino acid glycine group to replace the 4-piperidinopiperidine group to overcome the metabolism drawback of CPT-11. Then by conjugating the amino group of glycine to the 10-position of SN38 via a carbamate bond, the carboxyl group of ZBH-01 converted to sodium

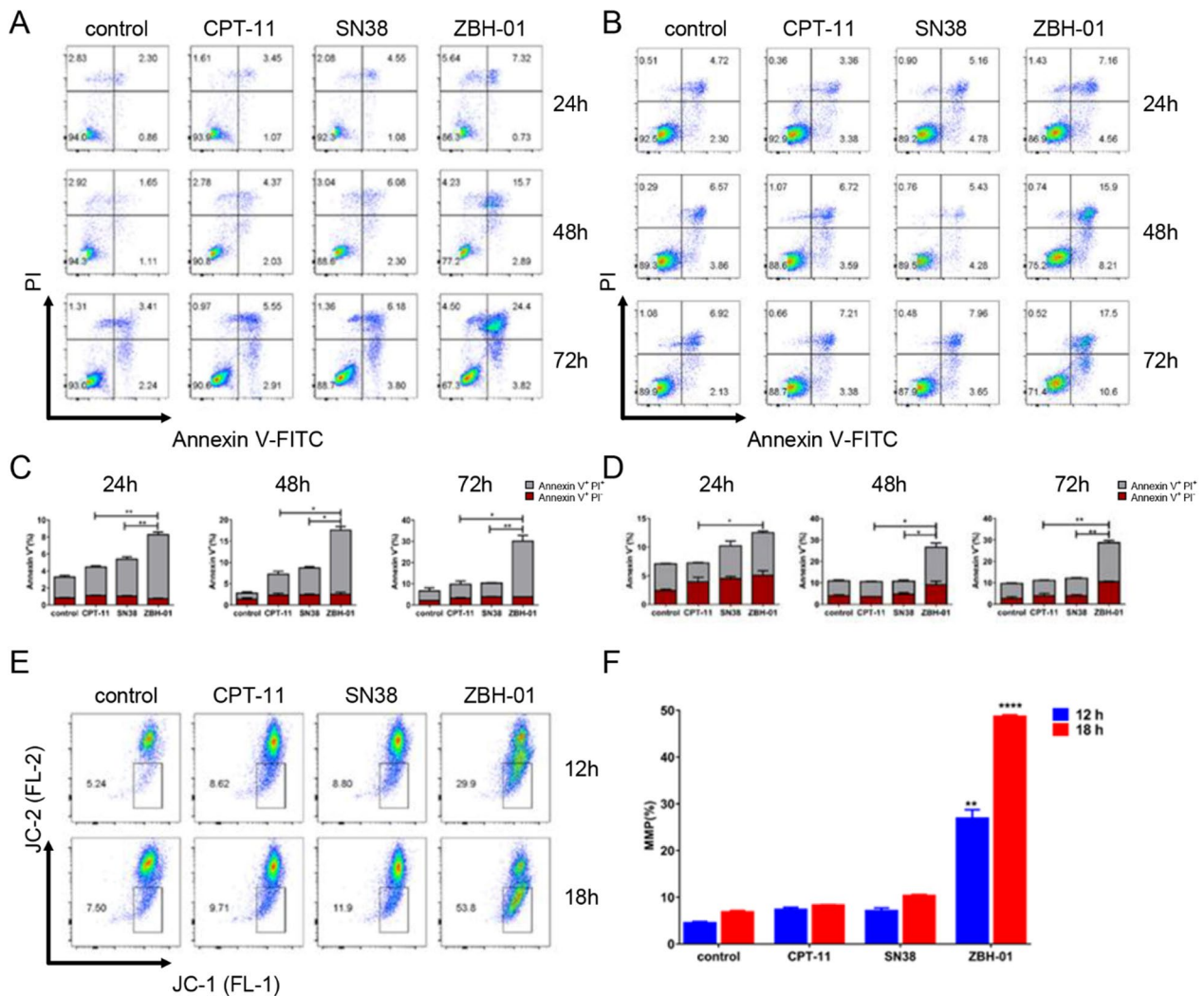


Fig. 7 Induction of tumor cell apoptosis by ZBH-01, CPT-11, and SN38 (50 nmol/l, 24 h). **A** Scatter diagrams of apoptosis of SW1116 cells at different times. **B** Statistical analysis of **A**. Annexin V⁺/PI⁻ (%), 12 h: **p*=0.0176, ZBH-01 vs. CPT-11. 48 h: **p*=0.0284, ZBH-01 vs. CPT-11. 72 h: ***p*=0.0047, ZBH-01 vs. CPT-11; ***p*=0.0067, ZBH-01 vs. SN38. ANOVA & two-tailed t-test, *n*=3. **C** Scatter diagrams of apoptosis of LS174T cells at different times. **D** Statistical analysis of **C**. Annexin V⁺/PI⁻ (%), 12 h: **p*=0.0148, ZBH-01 vs. CPT-11; **p*=0.0124, ZBH-01 vs. SN38. 18 h: **p*=0.0341, ZBH-01 vs. CPT-11; **p*=0.0374, ZBH-01 vs. SN38. 24 h: **p*=0.0404, ZBH-01 vs. CPT-11; **p*=0.0299, ZBH-01 vs. SN38. 48 h: **p*=0.0399, ZBH-01 vs. SN38. 72 h: **p*=0.0073, ZBH-01 vs. CPT-11; ***p*=0.0070, ZBH-01 vs. SN38. ANOVA & two-tailed t-test, *n*=3. **E** Scatter diagrams of MMP of LS174T cells in response to drug treatment (50 nmol/l) at different time points. **F** Statistical analysis of **E**. 12 h: **p*=0.0178, ZBH-01 vs. SN38. 18 h: ***p*=0.0047, ZBH-01 vs. CPT-11; ***p*=0.0047, ZBH-01 vs. SN38. 24 h: *****p*<0.0001, ZBH-01 vs. CPT-11; *****p*<0.0001, ZBH-01 vs. SN38. ANOVA & two-tailed t-test, *n*=2

salt to improve its water solubility. ZBH-01 showed more potent antitumor activity in vitro even in the CPT-11-resistant cells. The 3D cell culture and in vivo xenograft model further confirmed superior anti-tumorigenesis effect of ZBH-01 than CPT-11 and SN38. ZBH-01 can rapidly convert to SN38 in both non-enzymatic physiological buffer (pH 7.4) and plasma in vitro. Its AChE inhibition activity and in vivo toxicity was also lower than that of CPT-11. All these characteristics of ZBH-01 might contribute to its antitumor potency.

We next compared the inhibitory effects of ZBH-01 and CPT-11/SN38 on TOP1 in colon cancer cells. The DNA relaxation assay unexpectedly showed that the inhibition of ZBH-01 on TOP1 was significantly lower than CPT-11 and SN38. This was inconsistent with our previous reports [9, 11]. However, the result of ICE bioassay showed that the inhibitory ability of ZBH-01 to TOP1 through chromatin-associated TOP cleavage complexes is higher than that of CPT-11 and SN38. We then confirmed this effect by NGS and qRT-PCR. Western blot

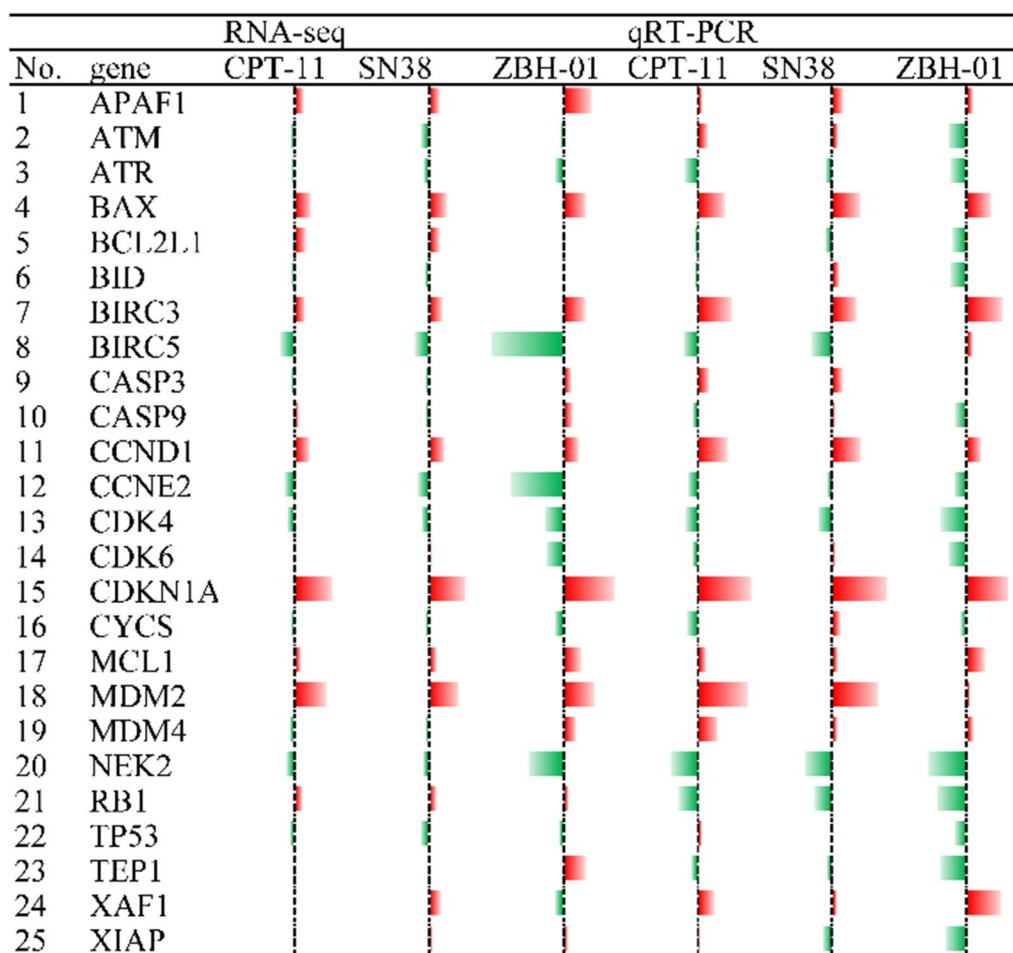


Fig. 8 Relative mRNA expression of some differentially expressed genes involved in apoptosis in LS174T cells after treatment with 50 nmol/L ZBH-01, CPT-11, and SN38 24 h (logarithmic transformation). Green, downregulated; Red, upregulated

result showed that TOP1 protein was slightly downregulated by ZBH-01, suggesting that ZBH-01 might inhibit TOP1 after transcription. Unexpectedly, we observed that the TOP2A mRNA level were significantly repressed in the ZBH-01 group by NGS and qRT-PCR. This might be related to the chemical structure of ZBH-01. We intend to explore this issue in the future.

High-throughput-based gene expression profiling enables characterization of drug sensitivity of tumor cells [38] and identification of new drug targets [21]. We compared mRNA expression profiles of colon cancer cells treated with ZBH-01, CPT-11, and SN38, respectively. The results showed that ZBH-01 treatment remarkably induced a unique abnormal expression of 1769 DEMRNAs (842 downregulated and 927 upregulated mRNAs) in LS174T cells. These DEMRNAs were mainly enriched in DNA replication, p53 signaling pathway, and cell cycle. After filtered out one prominent module from the PPI network, we found that the 73 genes in the

module mostly associated with the cell cycle. Interestingly, TOP2A was also located at the center of the module, which again reminds us of its importance.

We then performed cell cycle and apoptosis assays to confirm the antitumor activity of ZBH-01. Under the same conditions (50 nmol/L, 24 h), ZBH-01 significantly induced more apoptosis and cell cycle arrest in the G₁ phase in LS174T and SW1116 colon cancer cells; while CPT-11 and SN38 mainly induced cell cycle arrest in the S phase. Even after treatment 48 and 72 h, CPT-11 and SN38 did not induce apparent apoptosis. Furthermore, ZBH-01 presenting a stronger effect on inducing tumor cell apoptosis at 12 and 18 h earlier. These results were additionally verified by the MMP and western blot assay [39] and are consistent with others' report that increasing expression of p53 after CPT treatment leading to cell cycle arrest [40], and CPT-11 inducing cell cycle arrest in the S- and G₂/M-phases [20, 41]. γ-H2AX, BRCA1, CHK1, CHK2, and P53 are key regulators in

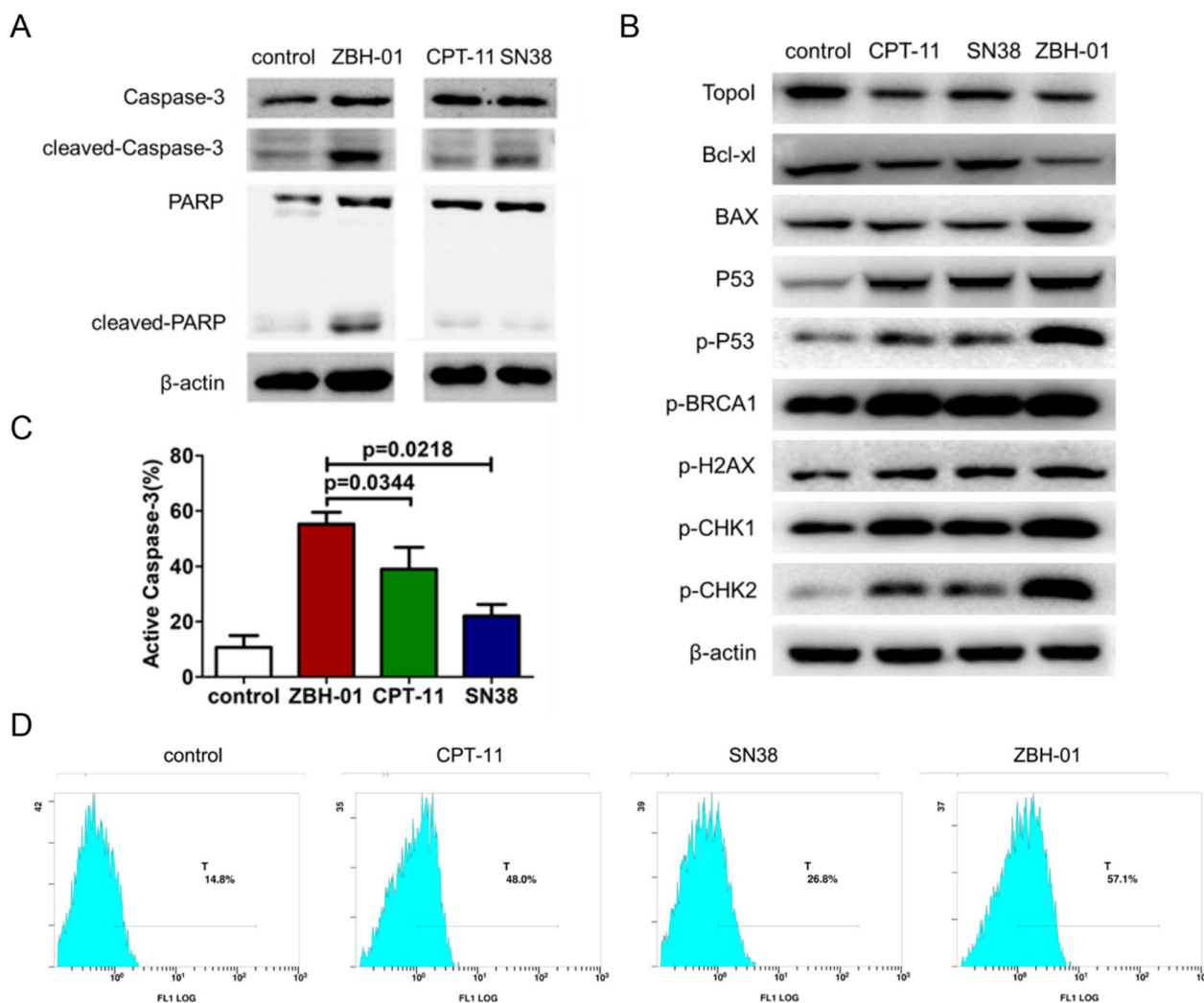


Fig. 9 The alternative expression of some key proteins related to cell apoptosis and DNA damage in LS174T cells after treatment with ZBH-01, CPT-11, and SN38 (50 nmol/l, 24 h), respectively. **A, B** The result of western blot showed that ZBH-01 is more efficient than CPT-11 and SN38 in regulating the expression of representative proteins. **C** Histogram of statistical analysis showed the active caspase-3 level in LS174T cells after treatment with ZBH-01, CPT-11, and SN38 (50 nmol/l, 24 h), respectively. **D** Representative graph showed the active caspase-3 percentage detected by flow cytometry in LS174T cells. ANOVA & two-tailed t-test, n = 3

various signaling pathways including DNA damage, cell cycle, and apoptosis [42]. Our results showed that ZBH-01 treatment increased the expression of p-BRCA1, p-H2AX, p-CHK1, p-CHK2, and p-P53 as compare with CPT-11 and SN38, which indicates that ZBH-01 promises more efficient activity in DNA damage. Altogether, these results might explain that ZBH-01 induced more extent of DNA damage than CPT-11 and SN38. Subsequently, it facilitates cell cycle arrest by causing the interaction between CCNA2, CDK2, and MYBL2, and promotes cell apoptosis by regulating the expression of apoptosis-related genes (Fig. 11).

Our study has some limitations. First, we should analyze more tumor cell lines and other tumor models in mice. Second, we only verified the levels of some DEmRNAs by qRT-PCR. Neither the expressions of gene-encoded proteins nor the gain of or loss of function was evaluated. Furthermore, we did not add corresponding agonists or antagonists to help investigate the mechanisms of ZBH-01. Additionally, there are actual differences between the expression patterns of DEmRNAs in colon cancer tissues and cell lines after drug treatments, and how to fully elucidate these differences might be considered in the future.

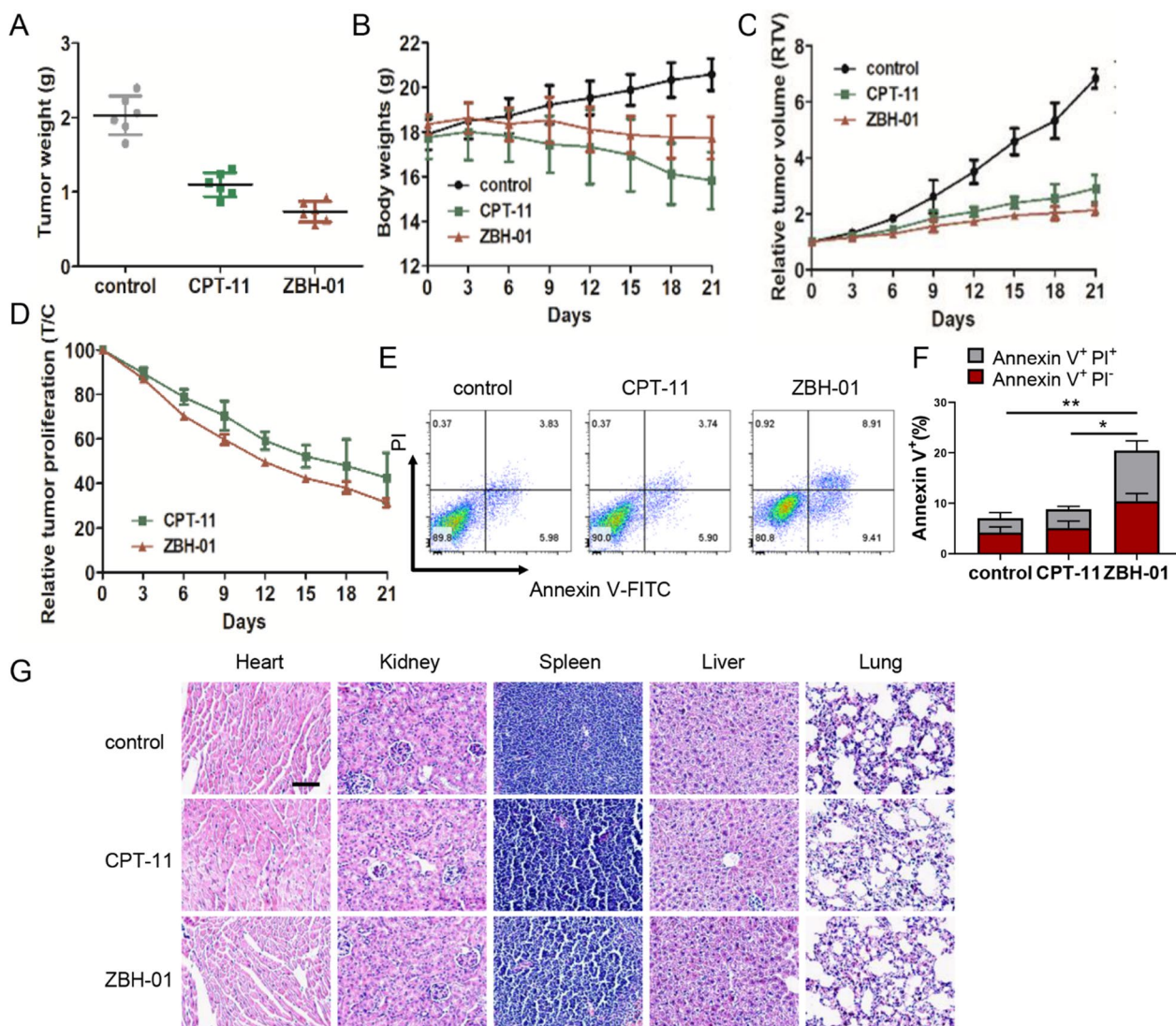


Fig. 10 In vivo antitumor activity of ZBH-01 and CPT-11 in colon cancer xenograft model in nude mice. **A** Tumor weights (g) at the end of the experiment. $***p < 0.0001$, CPT-11 vs. control, $***p < 0.0001$, ZBH-01 vs. control, $**p = 0.0019$, ZBH-01 vs. CPT-11. **B** Body weights (g) at various times. $***p = 0.0001$, CPT-11 vs. control, $**p = 0.0040$, ZBH-01 vs. control, $**p = 0.0057$, ZBH-01 vs. CPT-11. **C** Relative tumor volumes at various times. $p = 0.0724$, CPT-11 vs. control, $*p = 0.0380$, ZBH-01 vs. control, $p = 0.2056$, ZBH-01 vs. CPT-11. **D** Relative tumor proliferation at various time. $p = 0.5030$, ZBH-01 vs. CPT-11. ANOVA & t-test, two-tailed, $n = 6$. **E** The representative diagrams of cell apoptosis in vivo detected by flow cytometry. **F** Statistical analysis of E. $**p = 0.0027$, ZBH-01 vs. control, $*p = 0.0291$, CPT-11 vs. control, ANOVA & t-test, two-tailed, $n = 6$. **G** Representative H&E staining images of the major organs (Heart, Kidney, Spleen, Liver, and Lung) in the control, CPT-11 and ZBH-01 treatment group. Scale bar = 20 μm

Irinotecan has conspicuous advantages in the treatment of refractory metastatic colorectal cancer. It usually combined with other drugs in clinical scenes. AXEPT, a multicenter randomised phase III trial presented for the first time that the combination of capecitabine and irinotecan is effective and well tolerated in patients with advanced colorectal cancer [43]. CinClare is the first phase III trial using irinotecan combined with neoadjuvant radiochemotherapy for locally advanced rectal cancer treatment under the guidance of UGT1A1

genotype. The results show that the combined regimen with irinotecan significantly increased complete tumor response in Chinese patients [44]. Antibody drug conjugates (ADC) are a new type of biological drugs which conjugate monoclonal antibody and cytotoxic small molecule drugs through bioactive linkers [45]. Two FDA-approved ADCs, Enhertu (DS-8201) and Sacituzumab govitecan (IMMU132), are both designed based on irinotecan with SN38 as loading drug [46–48]. The new compound ZBH-01 was designed to reduce the severe

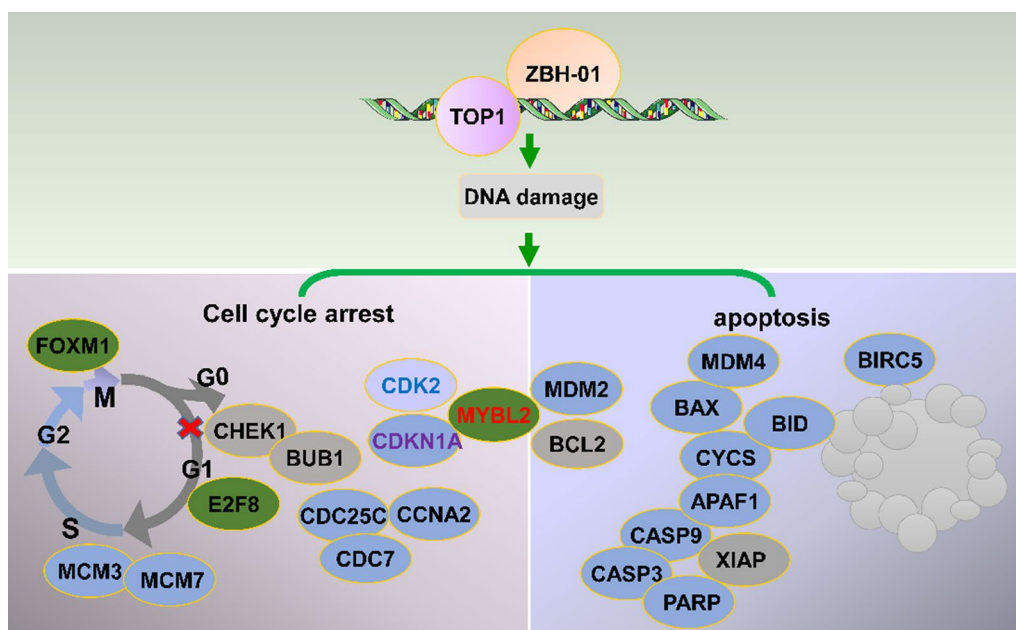


Fig. 11 Hypothetical ZBH-01 mechanisms. The DNA damage caused by ZBH-01 induces not only cell cycle arrest but also apoptosis. CCNA2, CDK2, MYBL2, CHEK1, BAX, BCL2L1, caspase 3, and other genes might be regulated by ZBH-01

side effects of irinotecan and improve it in vivo conversion efficiency to SN38. Theoretically, ZBH-01 has the potential to be used in any scenario where irinotecan can be applied. We need to investigate whether the combination of ZBH-01 and other drugs can improve the clinical response in the future.

Abbreviation

BUB	BUB1 mitotic checkpoint serine/threonine kinase
BUB1B	BUB1 mitotic checkpoint serine/threonine kinase B
CCNA2	Cyclin A2
CDC20	Cell division cycle 20
CDC25C	Cell division cycle 25C
CDC45	Cell division cycle 45
CDC7	Cell division cycle 7
CDK2	Cyclin dependent kinase 2
CHEK1 (CHK1)	Checkpoint kinase 1
E2F8	E2F transcription factor 8
EZH2	Enhancer of zeste 2 polycomb repressive complex 2 subunit
FOXM1	Forkhead box M1
MCM3	Minichromosome maintenance complex component 3
MCM7	Minichromosome maintenance complex component 7
MYBL2	MYB proto-oncogene like 2
ORC1	Origin recognition complex subunit 1
PKMYT1	Protein kinase, membrane associated tyrosine/threonine 1
RAD54L	RAD54 like
TOP1	DNA topoisomerase I
TOP2A	DNA topoisomerase II alpha
TTK	TTK protein kinase
APAF1	Apoptotic peptidase activating factor 1
ATM	Ataxia telangiectasia mutated
ATR	Ataxia telangiectasia related
BAX	BCL2 associated X, apoptosis regulator
BCL2L1	BCL2 like 1
BID	BH3 interacting domain death agonist

BIRC3 (c-IAP2)	Baculoviral IAP repeat containing 3
BIRC5 (survivin)	Baculoviral IAP repeat containing 5
CASP3	Caspase 3
CASP9	Caspase 9
CCND1	Cyclin D1
CCNE2	Cyclin E2
CDK4	Cyclin dependent kinase 4
CDK6	Cyclin dependent kinase 6
CDKN1A (P21)	Cyclin dependent kinase inhibitor 1A
CYCS	Cytochrome c, somatic
MCL1	MCL1 apoptosis regulator, BCL2 family member
MDM2	MDM2 proto-oncogene
MDM4	MDM4 regulator of p53
NEK2	NIMA related kinase 2
RB1	RB transcriptional corepressor 1
TP53	Tumor protein p53
TEP1	Telomerase associated protein 1
XAF1	XIAP associated factor 1
XIAP (BIRC4)	X-linked inhibitor of apoptosis
PARP	Poly-ADP-ribose-polymerase

Acknowledgements

We thank Prof Hubing Shi and Dr. Jing Yu from Sichuan University for assistance with bioinformatic analysis.

Author contributions

YL designed and performed most of the experiments; HY conceived of the study and wrote the manuscript; MY and ZW conducted qRT-PCR; DZ and WZ contributed to the DNA relaxation assay; SL and ZG assist in in vivo experiments; ZT provided reagents; WS synthesized and provided ZBH-01. DW and HY supervised all aspects of the study. All authors read and approved the final manuscript.

Funding

The present study was supported by funding of the Natural Science Foundation of Jilin Province (to DW, Grant No. 20200201479JC).

Availability of data and materials

All data and materials related in this research are available for sharing.

Declarations

Ethics approval and consent to participate

The study was approved by the Institutional Review Board (IRB) of The First Hospital of Jilin University. All subjects were provided a written informed consent.

Consent for publication

I give my consent for the article to publish in Journal of translational medicine, section of tumor chemotherapy.

Competing interests

The authors declare that they have no competing of interest.

Author details

¹Department of Cancer Centre, The First Hospital of Jilin University, Changchun 130021, China. ²Institute of Translational Medicine, The First Hospital of Jilin University, Changchun 130061, China. ³Department of Breast Tumor, Jilin Cancer Hospital, Changchun 130012, China. ⁴Institute of Pharmacology and Toxicology Academy of Military Medical Sciences, Beijing 100850, China. ⁵Cell Biology Laboratory, Jilin Province Institute of Cancer Prevention and Treatment, Jilin Cancer Hospital, Changchun 130012, China.

Received: 23 June 2022 Accepted: 14 May 2023

Published online: 29 June 2023

References

- Feng RM, Zong YN, Cao SM, Xu RH. Current cancer situation in China: good or bad news from the 2018 global cancer statistics? *Cancer Commun*. 2019;39:22. <https://doi.org/10.1186/s40880-019-0368-6>.
- Chen W, Zheng R, Baade PD, Zhang S, Zeng H, Bray F, Jemal A, Yu XQ, He J. Cancer statistics in China, 2015. *CA Cancer J Clin*. 2016;66:115–32. <https://doi.org/10.3322/caac.21338>.
- Fujita K-i, Kubota Y, Ishida H, Sasaki Y. Irinotecan, a key chemotherapeutic drug for metastatic colorectal cancer. *World J Gastroenterol*. 2015;21:12234–48.
- Thomas A, Pommier Y. Targeting Topoisomerase I in the Era of Precision Medicine. *Clin Cancer Res*. 2019;25:6581–9. <https://doi.org/10.1158/1078-0432.CCR-19-1089>.
- Pommier Y. Drugging topoisomerases: lessons and challenges. *ACS Chem Biol*. 2013;8:82–95. <https://doi.org/10.1021/cb300648v>.
- Li F, Jiang T, Li Q, Ling X. Camptothecin (CPT) and its derivatives are known to target topoisomerase I (Top1) as their mechanism of action: did we miss something in CPT analogue molecular targets for treating human disease such as cancer? *Am J Cancer Res*. 2017;7:2350–94.
- Yuan J-M, Chen N-Y, Liao H-R, Zhang G-H, Li X-J, Gu Z-Y, Pan C-X, Mo D-L, Su G-F. 3-(Benzo[d]thiazol-2-yl)-4-aminoquinoline derivatives as novel scaffold topoisomerase I inhibitor via DNA intercalation: design, synthesis, and antitumor activities. *New J Chem*. 2020;44:11203–14. <https://doi.org/10.1039/C9NJ05846J>.
- Foto E, Özen Ç, Zilifdar F, Tekiner-Gülbaş B, Yıldız İ, Aki-Yalçın E, Diril N, Yalçın İ. Benzoxazines as new human topoisomerase I inhibitors and potential poisons. *DARU J Pharm Sci*. 2020;28:65–73. <https://doi.org/10.1007/s40199-019-00315-x>.
- Wu D, Shi W, Zhao J, Wei Z, Chen Z, Zhao D, Lan S, Tai J, Zhong B, Yu H. Assessment of the chemotherapeutic potential of a new camptothecin derivative, ZBH-1205. *Arch Biochem Biophys*. 2016;604:74–85. <https://doi.org/10.1016/j.abb.2016.06.007>.
- Zhou M, Liu M, He X, Yu H, Wu D, Yao Y, Fan S, Zhang P, Shi W, Zhong B. Synthesis and biological evaluation of novel 10-substituted-7-ethyl-10-hydroxycamptothecin (SN-38) prodrugs. *Molecules*. 2014;19:19718–31. <https://doi.org/10.3390/molecules191219718>.
- Wu D, Zhao DW, Li YQ, Shi WG, Yin QL, Tu ZK, Yu YY, Zhong BH, Yu H, Bao WG. Antitumor potential of a novel camptothecin derivative, ZBH-ZM-06. *Oncol Rep*. 2018;39:871–9. <https://doi.org/10.3892/or.2017.6143>.
- Zhao D, Wu D, Zhang G, Li Y, Shi W, Zhong B, Yu H. A novel irinotecan derivative ZBH-1207 with different anti-tumor mechanism from CPT-11 against colon cancer cells. *Mol Biol Rep*. 2022;49:8359–68. <https://doi.org/10.1007/s11033-022-07652-2>.
- Livak KJ, Schmittgen TD. Analysis of relative gene expression data using real-time quantitative PCR and the 2(-Delta Delta C(T)) method. *Methods*. 2001;25:402–8. <https://doi.org/10.1006/meth.2001.1262>.
- Pourquier P, Takebayashi Y, Urasaki Y, Gioffre C, Kohlhagen G, Pommier Y. Induction of topoisomerase I cleavage complexes by 1-beta-D-arabino-furanosylcytosine (ara-C) in vitro and in ara-C-treated cells. *Proc Natl Acad Sci U S A*. 2000;97:1885–90. <https://doi.org/10.1073/pnas.97.4.1885>.
- Yu G, Wang L-G, Han Y, He Q-Y. clusterProfiler: an R package for comparing biological themes among gene clusters. *OMICS*. 2012;16:284–7. <https://doi.org/10.1089/omi.2011.0118>.
- Szklarczyk D, Franceschini A, Wyder S, Forslund K, Heller D, Huerta-Cepas J, Simonovic M, Roth A, Santos A, Tsafou KP, et al. STRING v10: protein-protein interaction networks, integrated over the tree of life. *Nucleic Acids Res*. 2015;43:D447–52. <https://doi.org/10.1093/nar/gku1003>.
- Shannon P, Markiel A, Ozier O, Baliga NS, Wang JT, Ramage D, Amin N, Schwikowski B, Ideker T. Cytoscape: a software environment for integrated models of biomolecular interaction networks. *Genome Res*. 2003;13:2498–504. <https://doi.org/10.1101/gr.1239303>.
- Li D-Z, Zhang Q-Z, Wang C-Y, Zhang Y-L, Li X-Y, Huang J-T, Liu H-Y, Fu Z-D, Song H-X, Lin J-P, et al. Synthesis and antitumor activity of novel substituted uracil-1'(N)-acetic acid ester derivatives of 20(S)-camptothecins. *Eur J Med Chem*. 2017;125:1235–46. <https://doi.org/10.1016/j.ejmech.2016.11.013>.
- Cincinelli R, Musso L, Artali R, Guglielmi MB, La Porta I, Melito C, Colelli F, Cardile F, Signorino G, Fucci A, et al. Hybrid topoisomerase I and HDAC inhibitors as dual action anticancer agents. *PLoS ONE*. 2018;13:e0205018–e0205018. <https://doi.org/10.1371/journal.pone.0205018>.
- Zou J, Li S, Chen Z, Lu Z, Gao J, Zou J, Lin X, Li Y, Zhang C, Shen L. A novel oral camptothecin analog, gimitecan, exhibits superior antitumor efficacy than irinotecan toward esophageal squamous cell carcinoma in vitro and in vivo. *Cell Death Dis*. 2018;9:e661. <https://doi.org/10.1038/s41419-018-0700-0>.
- Barretina J, Caponigro G, Stransky N, Venkatesan K, Margolin AA, Kim S, Wilson CJ, Lehár J, Kryukov GV, Sonkin D, et al. The cancer cell line encyclopedia enables predictive modelling of anticancer drug sensitivity. *Nature*. 2012;483:603–7. <https://doi.org/10.1038/nature11003>.
- Mariadason JM, Arango D, Shi Q, Wilson AJ, Corner GA, Nicholas C, Aranes MJ, Lesser M, Schwartz EL, Augenlicht LH. Gene expression profiling-based prediction of response of colon carcinoma cells to 5-fluorouracil and camptothecin. *Cancer Res*. 2003;63:8791–812.
- Lalève S, Feil R. Long noncoding RNAs in human disease: emerging mechanisms and therapeutic strategies. *Epigenomics*. 2015;7:877–9. <https://doi.org/10.2217/epi.15.55>.
- Szklarczyk D, Morris JH, Cook H, Kuhn M, Wyder S, Simonovic M, Santos A, Doncheva NT, Roth A, Bork P, et al. The STRING database in 2017: quality-controlled protein-protein association networks, made broadly accessible. *Nucleic Acids Res*. 2017;45:D362–8. <https://doi.org/10.1093/nar/gkw937>.
- Bader GD, Hogue CW. An automated method for finding molecular complexes in large protein interaction networks. *BMC Bioinformatics*. 2003;4:2. <https://doi.org/10.1186/1471-2105-4-2>.
- Müller-Tidow C, Wang W, Idos GE, Diederichs S, Yang R, Readhead C, Berdel WE, Serve H, Saville M, Watson R, Koeffler HP. Cyclin A1 directly interacts with B-myb and cyclin A1/cdk2 phosphorylate B-myb at functionally important serine and threonine residues: tissue-specific regulation of B-myb function. *Blood*. 2001;97:2091–7. <https://doi.org/10.1182/blood.V97.7.2091>.
- Tripathi V, Shen Z, Chakraborty A, Giri S, Freier SM, Wu X, Zhang Y, Gorospe M, Prasanth SG, Lal A, Prasanth KV. Long noncoding RNA MALAT1 controls cell cycle progression by regulating the expression of oncogenic transcription factor B-MYB. *PLoS Genet*. 2013;9:e1003368–e1003368. <https://doi.org/10.1371/journal.pgen.1003368>.
- Bartsch O, Horstmann S, Toprak K, Klempnauer K-H, Ferrari S. Identification of cyclin A/Cdk2 phosphorylation sites in B-Myb. *Eur J Biochem*. 1999;260:384–91. <https://doi.org/10.1046/j.1432-1327.1999.00191.x>.
- Tian Y, Chen H, Qiao L, Zhang W, Zheng J, Zhao W, Chen JJ, Zhang W. CIP2A facilitates the G1/S cell cycle transition via B-Myb in human papillomavirus 16 oncoprotein E6-expressing cells. *J Cell Mol Med*. 2018;22:4150–60. <https://doi.org/10.1111/jcmm.13693>.

30. Bessa M, Saville MK, Watson RJ. Inhibition of cyclin A/Cdk2 phosphorylation impairs B-Myb transactivation function without affecting interactions with DNA or the CBP coactivator. *Oncogene*. 2001;20:3376–86. <https://doi.org/10.1038/sj.onc.1204439>.
31. Petrovas C, Jeay S, Lewis RE, Sonenshein GE. B-Myb repressor function is regulated by cyclin A phosphorylation and sequences within the C-terminal domain. *Oncogene*. 2003;22:2011–20. <https://doi.org/10.1038/sj.onc.1206231>.
32. Guan Z, Cheng W, Huang D, Wei A. High MYBL2 expression and transcription regulatory activity is associated with poor overall survival in patients with hepatocellular carcinoma. *Curr Res Transl Med*. 2018;66:27–32. <https://doi.org/10.1016/j.retram.2017.11.002>.
33. Pommier Y, Sun Y, Huang SN, Nitiss JL. Roles of eukaryotic topoisomerases in transcription, replication and genomic stability. *Nat Rev Mol Cell Biol*. 2016;17:703–21. <https://doi.org/10.1038/nrm.2016.111>.
34. Bailly C. Irinotecan: 25 years of cancer treatment. *Pharmacol Res*. 2019;148:104398. <https://doi.org/10.1016/j.phrs.2019.104398>.
35. Takaoka T, Kimura T, Shimoyama R, Kawamoto S, Sakamoto K, Goda F, Miyamoto H, Negoro Y, Tsuji A, Yoshizaki K, et al. Panitumumab in combination with irinotecan plus S-1 (IRIS) as second-line therapy for metastatic colorectal cancer. *Cancer Chemother Pharmacol*. 2016;78:397–403. <https://doi.org/10.1007/s00280-016-3096-5>.
36. Yang XY, Zhao HY, Lei H, Yuan B, Mao S, Xin M, Zhang SQ. Synthesis and biological evaluation of 10-substituted camptothecin derivatives with improved water solubility and activity. *ChemMedChem*. 2020;16:1000–10. <https://doi.org/10.1002/cmdc.202000753>.
37. Chen Z, Liu Z, Huang W, Li Z, Zou J, Wang J, Lin X, Li B, Chen D, Hu Y, et al. Gimitecan exerts potent antitumor activity against gastric cancer in vitro and in vivo via AKT and MAPK signaling pathways. *J Transl Med*. 2017;15:253–253. <https://doi.org/10.1186/s12967-017-1360-z>.
38. Arroyo MM, Berral-González A, Bueno-Fortes S, Alonso-López D, Rivas JDL. Mining drug-target associations in cancer: analysis of gene expression and drug activity correlations. *Biomolecules*. 2020;10:667. <https://doi.org/10.3390/biom10050667>.
39. Czabotar PE, Lessene G, Strasser A, Adams JM. Control of apoptosis by the BCL-2 protein family: implications for physiology and therapy. *Nat Rev Mol Cell Biol*. 2014;15:49–63. <https://doi.org/10.1038/nrm3722>.
40. Cliby WA, Lewis KA, Lilly KK, Kaufmann SH. S Phase and G2 arrests induced by topoisomerase I poisons are dependent on ATR kinase function. *J Biol Chem*. 2002;277:1599–606. <https://doi.org/10.1074/jbc.M106287200>.
41. Maurya DK, Ayuzawa R, Doi C, Troyer D, Tamura M. Topoisomerase I inhibitor SN-38 effectively attenuates growth of human non-small cell lung cancer cell lines in vitro and in vivo. *J Environ Pathol, Toxicol Oncol*. 2011;30:1–10. <https://doi.org/10.1615/jenvironpatholtoxiconcol.v30.i1.10>.
42. Chen J. The cell-cycle arrest and apoptotic functions of p53 in tumor initiation and progression. *Cold Spring Harb Perspect Med*. 2016;6:a026104–a026104. <https://doi.org/10.1101/cshperspect.a026104>.
43. Xu RH, Muro K, Morita S, Iwasa S, Han SW, Wang W, Kotaka M, Nakamura M, Ahn JB, Deng YH, et al. Modified XELIRI (capecitabine plus irinotecan) versus FOLFIRI (leucovorin, fluorouracil, and irinotecan), both either with or without bevacizumab, as second-line therapy for metastatic colorectal cancer (AXEPT): a multicentre, open-label, randomised, non-inferiority, phase 3 trial. *Lancet Oncol*. 2018;19:660–71. [https://doi.org/10.1016/s1470-2045\(18\)30140-2](https://doi.org/10.1016/s1470-2045(18)30140-2).
44. Zhu J, Liu A, Sun X, Liu L, Zhu Y, Zhang T, Jia J, Tan S, Wu J, Wang X, et al. Multicenter, randomized, phase III trial of neoadjuvant chemoradiation with capecitabine and irinotecan guided by UGT1A1 status in patients with locally advanced rectal cancer. *J Clin Oncol*. 2020;38:4231–9. <https://doi.org/10.1200/jco.20.01932>.
45. Talukdar A, Kundu B, Sarkar D, Goon S, Mondal MA. Topoisomerase I inhibitors: challenges, progress and the road ahead. *Eur J Med Chem*. 2022;236:114304. <https://doi.org/10.1016/j.ejmech.2022.114304>.
46. Khaiwa N, Maarouf NR, Darwish MH, Alhamad DWM, Sebastian A, Hamad M, Omar HA, Orive G, Al-Tel TH. Camptothecin's journey from discovery to WHO essential medicine: fifty years of promise. *Eur J Med Chem*. 2021;223:113639. <https://doi.org/10.1016/j.ejmech.2021.113639>.
47. Thomas A, Pommier Y. Targeting topoisomerase I in the era of precision medicine. *Clin Cancer Res*. 2019;25:6581–9. <https://doi.org/10.1158/1078-0432.Ccr-19-1089>.
48. Cardillo TM, Govindan SV, Sharkey RM, Trisal P, Arrojo R, Liu D, Rossi EA, Chang CH, Goldenberg DM. Sacituzumab govitecan (IMMU-132), an anti-Trop-2/SN-38 antibody-drug conjugate: characterization and efficacy in pancreatic, gastric, and other cancers. *Bioconjug Chem*. 2015;26:919–31. <https://doi.org/10.1021/acs.bioconjchem.5b00223>.

Publisher's Note

Springer Nature remains neutral with regard to jurisdictional claims in published maps and institutional affiliations.

Ready to submit your research? Choose BMC and benefit from:

- fast, convenient online submission
- thorough peer review by experienced researchers in your field
- rapid publication on acceptance
- support for research data, including large and complex data types
- gold Open Access which fosters wider collaboration and increased citations
- maximum visibility for your research: over 100M website views per year

At BMC, research is always in progress.

Learn more biomedcentral.com/submissions

